

A COMPARISON OF ALTERNATIVE FILTERBANK MULTICARRIER METHODS FOR COGNITIVE RADIO SYSTEMS

Peiman Amini (University of Utah, Salt Lake City, UT, USA⁺; pamini@ece.utah.edu),
Roland Kempter (⁺; kempter@ece.utah.edu),
Behrouz Farhang-Boroujeny (⁺; farhang@ece.utah.edu)

ABSTRACT

We introduce and compare three filterbank-based communication methods for cognitive radio systems. In the first method, called Filtered Multitone (FMT), subcarriers are arranged such that adjacent subbands do not overlap. While this makes FMT robust to channel impairments, it leads to considerable losses in bandwidth efficiency. Next, we discuss orthogonal frequency division multiplexing with offset QAM (OFDM-OQAM). OFDM-OQAM operates based on quadrature amplitude modulated (QAM) symbols whose in-phase and quadrature components are time offset by half the symbol period. The third method, which is referred to as cosine modulated multitone (CMT), is based on cosine modulated filterbanks. In CMT, the subcarrier symbols are pulse amplitude and vestigial side-band (VSB) modulated. We present filter designs for all methods and show that OFDM-OQAM offers highest stopband attenuation for a fixed filter length and number of subcarriers.

1. INTRODUCTION

Spectrum sensing as well as data transmission is a challenging problem in cognitive radio (CR) systems. Since the Fast Fourier transform (FFT) may be used for spectral analysis as well as for modulation/demodulation, orthogonal frequency division multiplexing (OFDM) has been suggested as a candidate for multicarrier based CR systems [3]. However, OFDM has a number of shortcomings in the CR environment. For instance, Weiss *et al.* [3] have studied the mutual interference between primary and secondary users in an OFDM-based CR setting, and have shown that the reduction of such interference is only possible by sacrificing a significant portion of the transmission bandwidth. Furthermore, for reliable detection of spectrum holes, the channel sensing mechanism needs to feature a high spectral dynamic range. Unfortunately, the FFT as part of an OFDM data transmission system is neither able to fulfill this requirement [2], nor can it meet the FCC's envisioned out-of-band rejection specifications [5]. As a consequence, it is worthwhile to investigate alternative multicarrier/signal processing methods which can overcome the limitations of the FFT/OFDM. Recently, filterbank multitone has been proposed for CR systems for data transmission as well as channel sensing and it has been shown that filterbank multitone can serve as a near-optimal non-parametric spectrum analysis tool [1], [2].

Over the past three decades, three classes of filterbank-based multicarrier communication systems have been introduced. Saltzberg [7] was the first to propose a filterbank multicarrier communication system using a special quadrature amplitude modulation (QAM) technique. Prior research

that initiated this development was performed by Chang [6]. Developments in digital subscriber line (DSL) technologies led to two other classes of filterbank multicarrier communication systems; namely, filtered multitone (FMT) [10]- [12] and discrete wavelet multitone (DWMT) modulation [13]. Out of these, DWMT has been further developed recently and renamed cosine-modulated multitone (CMT), [14].

In the remainder of this paper, we present a tutorial review of FMT, CMT and OFDM-OQAM. Our intention is to introduce these three methods as alternative candidates to the widely studied conventional OFDM that suffers from significant leakage problems among different subcarrier bands [4]. A filter design is presented for all three methods.

2. FILTERED MULTITONE, FMT

In FMT, subcarriers are arranged such that adjacent subbands do not overlap. As such, FMT may be seen as a multicarrier communication technique that follows the principle of the legacy frequency division multiplexing (FDM) methodology to separate a high-rate data stream into a number of disjoint frequency bands. FMT's distinctive feature harnesses the fact that either all or at least a cluster of subcarriers are transmitted from the same source. Hence, those carriers can be synchronized and bundled together as one signal for transmission. Moreover, polyphase techniques can be used for efficient implementation. However, we note that in order to keep the subcarrier bands non-overlapping, excess bandwidth has to be reserved to allow for a transition band for each subcarrier.

In [10] and [12], where FMT was introduced for Digital Subscriber Line (DSL) technology, the width of the subcarrier transition band was kept at a minimum at the cost of signal distortion. To compensate, one decision feedback equalizer per subcarrier was required at the receiver, adding significant complexity. Moving from DSL to CR applications, we believe that the use of equalizers at the receiver may be impractical because of two technical reasons: (i) the added complexity may not be justifiable, particularly, when one can use CMT and/or OFDM-OQAM that offer higher bandwidth efficiency and lower complexity. (ii) It may be hard, if not impossible, to implement an adaptive equalizer (of the size mentioned in [12]) that can cope with the time variation of wireless channels. Consequently, we believe that in a CR setting, FMT will suffer from significant bandwidth loss due

to the large roll-off factors which have to be allowed in each subcarrier band.

3. OFDM-OQAM

In OFDM-OQAM, subcarrier bands are spaced by the symbol rate, $1/T$. In contrast to FMT, this results in significant overlap among adjacent bands. Successful signal separation is nevertheless possible thanks to a specific signaling arrangement. An introduced orthogonality condition between subcarriers guarantees that the transmitted symbols arrive at the receiver free of intersymbol (ISI) and intercarrier interference (ICI). Carrier orthogonality is achieved through time staggering the in-phase and quadrature components of the subcarrier symbols and designing proper transmit and receive filters. In this section, we elaborate on these aspects of OFDM-OQAM.

In a baseband equivalent of an OFDM-OQAM system as shown in Figure 1, N parallel complex data streams are passed to N subcarrier transmission filters. The in-phase and quadrature components are then staggered in time by half a symbol period, $T/2$. The outputs of these filters are then modulated using N subcarrier modulators whose carrier frequencies are $1/T$ -spaced apart.

Suppose that we have complex input symbols according to

$$x_k^n = a_k^n + jb_k^n \quad (1)$$

where a_k^n and b_k^n are the real and imaginary parts of the n th symbol, respectively. The complex-valued baseband OFDM-OQAM modulated signal is defined as

$$o(t) = \sum_{m=0}^{N-1} s_m(t) e^{jm(\frac{2\pi t}{T} + \frac{\pi}{2})} \quad (2)$$

where

$$s_m(t) = \sum_{l=-\infty}^{\infty} (a_l^m h(t-lT) + jb_l^m h(t-lT-T/2)). \quad (3)$$

Analogously, the output of the receiver, \hat{x}_k^n , consists of the real and imaginary components \hat{a}_k^n and \hat{b}_k^n ,

$$\hat{x}_k^n = \hat{a}_k^n + j\hat{b}_k^n. \quad (4)$$

In (4), \hat{a}_k^n is found as the real part of the signal at the output of the corresponding matched filter with response $h(t)$ and expressed as

$$\begin{aligned} \hat{a}_k^n &= \Re[h(-t) * p(t) |_{t=kT}] \\ &= \Re \left[\int_{-\infty}^{\infty} p(t) h(-(kT-t)) dt \right] \\ &= \Re \left[\int_{-\infty}^{\infty} h(t-kT) p(t) dt \right] \end{aligned} \quad (5)$$

where $*$ denotes convolution, and

$$p(t) = e^{-jn(\frac{2\pi t}{T} + \frac{\pi}{2})} o(t) \quad (6)$$

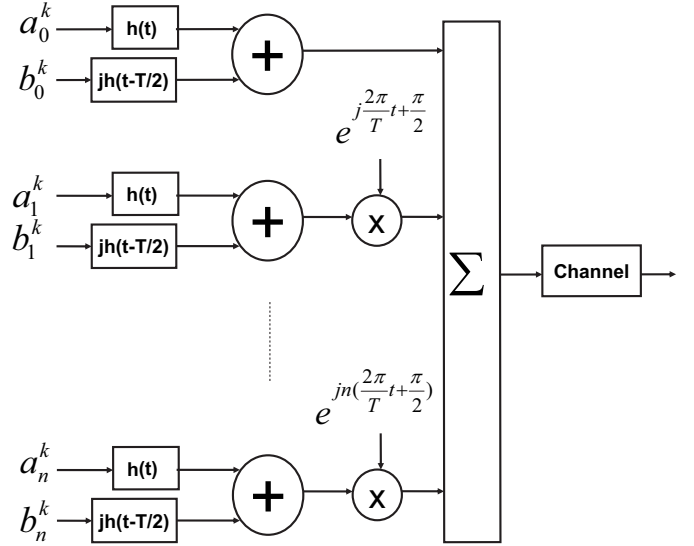


Fig. 1. Baseband OFDM-OQAM Transmitter

is the demodulated signal before matched filtering. Substituting (2) and (6) in (5), we obtain

$$\hat{a}_k^n = \Re \left[\int_{-\infty}^{\infty} h(t-kT) \sum_{m=0}^{N-1} s_m(t) e^{j(m-n)(\frac{2\pi t}{T} + \frac{\pi}{2})} dt \right]. \quad (7)$$

Furthermore, substituting (3) in (7), we get

$$\begin{aligned} \hat{a}_k^n &= \sum_{l=-\infty}^{\infty} \sum_{m=0}^{N-1} \int_{-\infty}^{\infty} \Re \left[h(t-kT) \left(a_l^m h(t-lT) \right. \right. \\ &\quad \left. \left. + jb_l^m h(t-lT-T/2) \right) e^{j(m-n)(\frac{2\pi t}{T} + \frac{\pi}{2})} \right] dt. \end{aligned} \quad (8)$$

This can be further rearranged as

$$\begin{aligned} \hat{a}_k^n &= \sum_{l=-\infty}^{\infty} \sum_{m=0}^{N-1} \int_{-\infty}^{\infty} \left[a_l^m h(t-kT) h(t-lT) \right. \\ &\quad \times \cos \left((m-n) \left(\frac{2\pi t}{T} + \frac{\pi}{2} \right) \right) \\ &\quad \left. - b_l^m h(t-kT) h(t-lT-T/2) \right. \\ &\quad \left. \times \sin \left((m-n) \left(\frac{2\pi t}{T} + \frac{\pi}{2} \right) \right) \right] dt. \end{aligned} \quad (9)$$

Changing the variable $t-kT$ to t and then taking into account

that l varies from $-\infty$ to ∞ , (9) can be simplified to

$$\begin{aligned} \hat{a}_k^n = & \sum_{l=-\infty}^{\infty} \sum_{m=0}^{N-1} a_{l+k}^n \int_{-\infty}^{\infty} \left[h(t-lT)h(t) \right. \\ & \times \cos \left((m-n) \left(\frac{2\pi t}{T} + \frac{\pi}{2} \right) \right) \\ & - b_{l+k}^n h(t-lT-T/2)h(t) \\ & \left. \times \sin \left((m-n) \left(\frac{2\pi t}{T} + \frac{\pi}{2} \right) \right) \right] dt. \end{aligned} \quad (10)$$

The block diagram of an OFDM-OQAM receiver performing these operations is depicted in Figure 2.

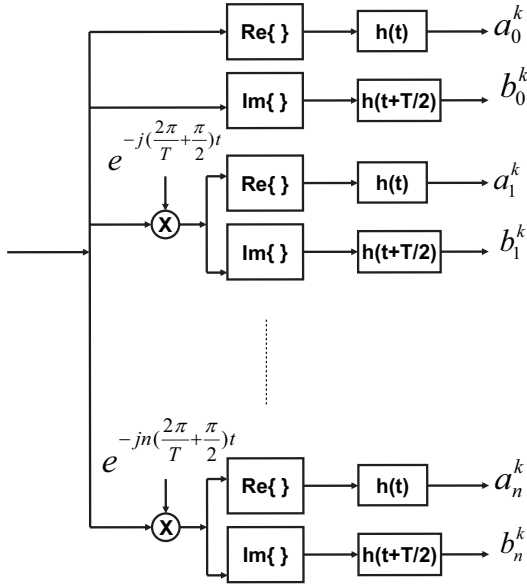


Fig. 2. Baseband OFDM-OQAM Receiver

Similarly, the imaginary part of the signal \hat{x}_k^n , \hat{b}_k^n can be found as

$$\hat{b}_k^n = \Im[h(-t-T/2) * p(t) |_{t=kT}]. \quad (11)$$

Starting with (11) and following the same line of derivations as above, we obtain

$$\begin{aligned} \hat{b}_k^n = & \sum_{l=-\infty}^{\infty} \sum_{m=0}^{N-1} \int_{-\infty}^{\infty} \left[a_{l+k}^n h(t-lT)h(t+T/2) \right. \\ & \times \sin \left((m-n) \left(\frac{2\pi t}{T} + \frac{\pi}{2} \right) \right) \\ & + b_{l+k}^n h(t-lT+T/2)h(t+T/2) \\ & \left. \times \cos \left((m-n) \left(\frac{2\pi t}{T} + \frac{\pi}{2} \right) \right) \right] dt. \end{aligned} \quad (12)$$

We now proceed to discuss the design of the matched filter, $h(t)$. In an ideal transmission system, the received signal equals the transmitted one and

$$\begin{aligned} \hat{a}_k^n &= a_k^n \\ \hat{b}_k^n &= b_k^n. \end{aligned} \quad (13)$$

It follows directly from (10) and (12), that (13) can be met, if $h(t)$ is chosen such that the equalities in (14)-(17) are satisfied. For convenience of the design, it is common to constrain $h(t)$ to a real and even (i.e., symmetric around $t = 0$) function of time, t . Under these constraints, one can show that the integrand in (15) is anti-symmetric around $t = lT/2 + T/4$ and the integrand in (16) is anti-symmetric around $t = lT/2 - T/4$. These, in turn, imply that (15) and (16) are automatically satisfied. Hence, in designing $h(t)$, it is sufficient to limit ourselves to the constraints imposed by (14) and (17). Also, to further simplify the design of $h(t)$, it is reasonable to assume that only adjacent subcarrier bands may overlap. When this is the case, only instances of m and n where $m-n = 0, +1, -1$ in (14) and (17) need to be considered. Values of m and n where $|m-n| > 1$ are related to non-adjacent subcarrier bands and thus, their multiplication in (14) results in values (close to) zero. Also, for $m-n = 0$, and iff $h(t)$ is a root-Nyquist filter, (14) equates to

$$\int_{-\infty}^{\infty} h(t-lT)h(t)dt = \delta(0,l) = \delta(l). \quad (18)$$

Finally, for $m-n = \pm 1$, (14) reduces to

$$\int_{-\infty}^{\infty} h(t-lT)h(t) \sin \left(\frac{2\pi t}{T} \right) dt = 0 \quad (19)$$

for any real and even choice of $h(t)$. In a similar way, and under the same conditions, one can show that (17) reduces to (18). In summary, any realization of $h(t)$ which is even and real and satisfies the root-Nyquist condition in (18), leads to an OFDM-OQAM transceiver system which satisfies (13). An example of such a design is given in Section 5-A.

4. COSINE MODULATED MULTITONE, CMT

Figure 3 presents the structure of a CMT multicarrier system. A synthesis filterbank is used to bandlimit a set of PAM symbols to vestigial sideband signals and modulate them to various frequency bands. This process is outlined graphically in Figure 4.

Fundamentally, vestigial sideband filtering is performed through a frequency shifted version of a lowpass filter $h(t)$, centered at $f = \pi/2T$ with impulse response $h(t)e^{j\frac{\pi}{2T}t}$. The transmit signal, corresponding to the positive part of the frequency axis, has the form

$$s_m^+(t) = \sum_k \left(\sum_n a_k^n h(t-nT) e^{j\frac{\pi}{2T}(t-nT)} \right) e^{j(\omega_k t + \theta_k)} \quad (20)$$

where ω_k s represents the carrier frequency of the k th subcarrier band and θ_k is a phase shift whose role will be explained below. We recall that while the transmit signal is $s_m(t) = \Re[s_m^+(t)]$, for the purpose of our discussion, we limit our attention to the use of $s_m^+(t)$.

To extract the k th subcarrier data sequence a_k^n , $s_m(t)$ is first multiplied by $e^{-j(\omega_k + \theta_k)t}$. The result is then passed

$$\int_{-\infty}^{\infty} h(t-lT)h(t) \cos\left((m-n)\left(\frac{2\pi t}{T} + \frac{\pi}{2}\right)\right) dt = \delta(m-n, l) \quad (14)$$

$$\int_{-\infty}^{\infty} h(t-lT-T/2)h(t) \sin\left((m-n)\left(\frac{2\pi t}{T} + \frac{\pi}{2}\right)\right) dt = 0 \quad (15)$$

$$\int_{-\infty}^{\infty} h(t-lT)h(t+T/2) \sin\left((m-n)\left(\frac{2\pi t}{T} + \frac{\pi}{2}\right)\right) dt = 0 \quad (16)$$

$$\int_{-\infty}^{\infty} h(t-lT+T/2)h(t+T/2) \cos\left((m-n)\left(\frac{2\pi t}{T} + \frac{\pi}{2}\right)\right) dt = \delta(m-n, l) \quad (17)$$

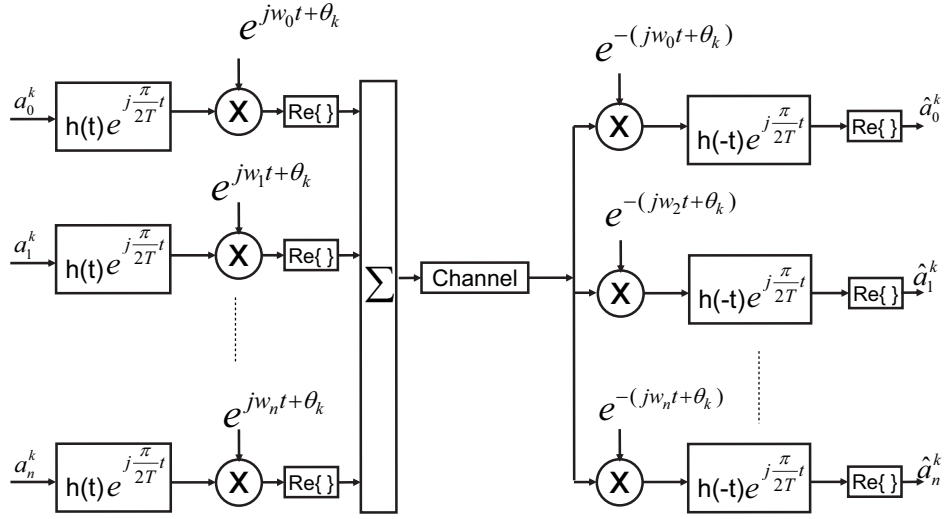


Fig. 3. Baseband CMT Trans-multiplexer

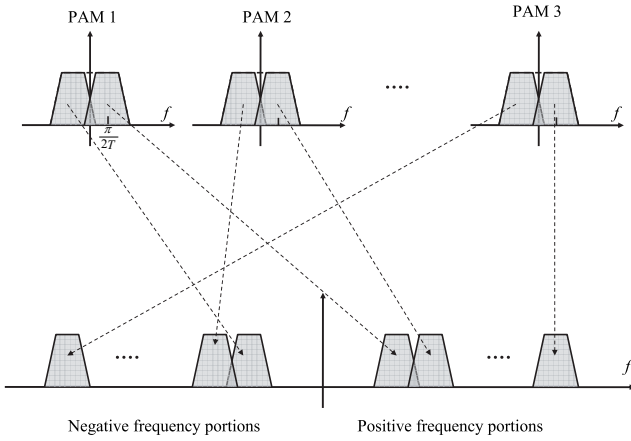


Fig. 4. CMT Modulation

through a lowpass filter, whose response is matched to the transmit filter $h(t)e^{j\frac{\pi}{2T}t}$, viz. $h(-t)e^{j\frac{\pi}{2T}t}$. Assuming that the matched filter has a high stopband attenuation, the matched filter output will only have three significant signal components. These components originate from the k th, $k+1$ th

and $k-1$ th subcarriers. Denoting the corresponding signal components by $y_i(t)$, $i = 0, +1, -1$, we have

$$y_i(t) = x_i(t) * h(-t)e^{j\frac{\pi}{2T}t} \quad (21)$$

where

$$x_0(t) = \left(\sum_n a_k^n h(t-nT) e^{j\frac{\pi}{2T}(t-nT)} \right), \quad (22)$$

$$x_1(t) = \left(\sum_n a_{k+1}^n h(t-nT) e^{j\frac{\pi}{2T}(t-nT)} \right) \times e^{j[(\omega_{k+1}-\omega_k)t+\theta_{k+1}-\theta_k]}, \quad (23)$$

and

$$x_{-1}(t) = \left(\sum_n a_{k-1}^n h(t-nT) e^{j\frac{\pi}{2T}(t-nT)} \right) \times e^{j[(\omega_{k-1}-\omega_k)t+\theta_{k-1}-\theta_k]}. \quad (24)$$

In CMT, the phase angle θ can be expressed as $\theta_k = (-1)^k \frac{\pi}{4}$ and the subcarrier bands are spaced $\omega_k - \omega_{k-1} = \pi/T$ apart.

Substituting these in the above set of equations, we get

$$x_1(t) = \pm j \left(\sum_n a_{k+1}^n h(t - nT) e^{j \frac{\pi}{2T}(t-nT)} \right) e^{j \frac{\pi}{T} t} \quad (25)$$

and

$$x_{-1}(t) = \mp j \left(\sum_n a_{k-1}^n h(t - nT) e^{j \frac{\pi}{2T}(t-nT)} \right) e^{j \frac{\pi}{T} t}. \quad (26)$$

Here, the $+$ or $-$ signs depend on k being either even or odd.

Using the above results, we obtain

$$\begin{aligned} y_0(t) &= \left(\sum_n a_k^n h(t - nT) e^{j \frac{\pi}{2T}(t-nT)} \right) * h(-t) e^{j \frac{\pi}{2T} t} \\ &= \sum_n a_k^n p(t - nT) e^{j \frac{\pi}{2T}(t-nT)} \end{aligned} \quad (27)$$

where $p(t) = h(t) * h(-t)$. We note that the complex signal at the output of the matched filter is centered at $\pi/2T$. Hence, taking the real part of the filter output results in the original signal, and sampling it at the time instants nT constitutes near-perfect reconstruction without any ISI.

Also, passing $x_1(t)$ through the matched filter $h(-t) e^{j \frac{\pi}{2T} t}$ results in

$$\begin{aligned} y_1(t) &= \pm j \left(\sum_n a_{k+1}^n h(t - nT) e^{j \frac{\pi}{2T}(t-nT)} \right) e^{j \frac{\pi}{T} t} \\ &\quad * h(-t) e^{j \frac{\pi}{2T} t} \\ &= \pm j \sum_n a_k^n q(t - nT) \end{aligned} \quad (28)$$

where $q(t) = h(t) e^{j \frac{\pi}{2T} t} e^{j \frac{\pi}{T} t} * h(-t) e^{j \frac{\pi}{2T} t}$ which can be calculated as

$$q(t) = e^{j \frac{\pi}{2T} t} \int_{-\infty}^{+\infty} h(\tau) h(\tau - t) e^{j \frac{\pi}{T} \tau} d\tau. \quad (29)$$

It is easy to show that $q(nT)$ is real. This in turn means that $y_1(t)$ is strictly imaginary, and thus has no effect on the output of the the CMT demodulator where the real part of the filter output is used only. In much the same way, one can show that $y_{-1}(t)$, too, is an imaginary number. As a result, with the chosen θ_k and ω_k , ICI can be avoided completely.

5. A COMPARISON OF FMT, OFDM-OQAM AND CMT

In OFDM-OQAM, each subcarrier band is double side-band modulated and carries a sequence of QAM (i.e., complex-valued) symbols. Opposed to this, in CMT, subcarrier modulation is vestigial sideband and the subcarriers carry a sequence of PAM (i.e., real-valued) symbols. Therefore, assuming identical symbol duration and number of sub-carriers, the CMT signal occupies half the bandwidth of OFDM-OQAM – of course, only providing half of its data rate. FMT, on the other hand, introduces guard bands between adjacent subcarriers which are complex modulated. The width of the

guardbands depends on the specific system implementation. Therefore, for an identical number of carriers and identical symbol timing, FMT requires more bandwidth than OFDM-OQAM and CMT. This relationship is shown in Figure 5.

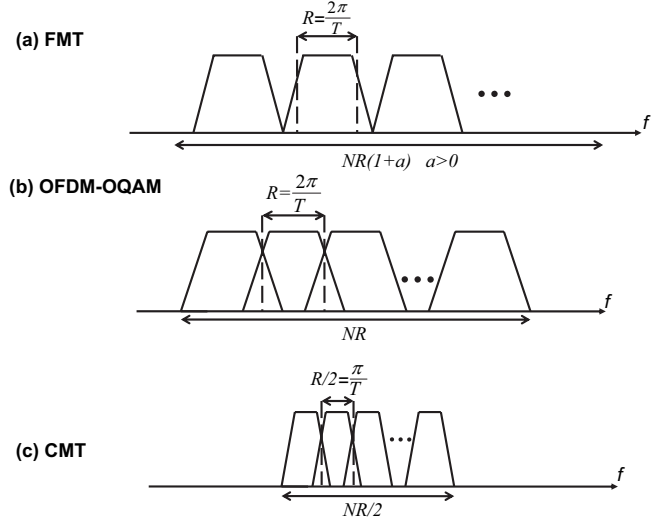


Fig. 5. Comparison between CMT, FMT and OFDM-OQAM

A. Numerical Results

In this section, we design filters for FMT, OFDM-OQAM, and CMT with a stopband attenuation of -60 dB for a multicarrier system with $N = 16$ subcarriers. We recall that while OFDM-OQAM filters are Nyquist N filters, CMT filters are Nyquist $2N$ filters. We assume identical roll-off factors of $\beta = 1$ for both, CMT and OQAM. In the case of FMT, we use a Nyquist N filter and assume a roll off factor of $\beta = 0.25$ to avoid losing more than 25% of bandwidth to guardbands. As the design method, we use an iterative least square algorithm [17]. The resulting filter responses are presented in Figure 6. With $N = 16$ subcarriers and a desired stopband attenuation of -60 dB, the required OFDM-OQAM filter length is $4N = 64$, the CMT filter length is $8N = 128$, and FMT requires a filter length of $16N = 256$. The reason why the filter length for CMT is twice that of OFDM-OQAM lies in the different bandwidth of the subcarriers, requiring half the transition band and thus twice the filter length in the case of CMT. However, as far as FMT is concerned, a roll-off factor of $\beta = 0.25$ results in a transition band which is 4 times smaller than that of OFDM-OQAM, hence requiring 4 times its filter length.

6. THE EFFECT OF THE CHANNEL ON FILTERBANK MULTICARRIER SYSTEMS

In conventional OFDM, a frequency selective channel can be converted into a number of subcarrier channels with the aid of the cyclic prefix. Each of these subcarrier channels can then be modeled as a flat channel, i.e., a channel that can be

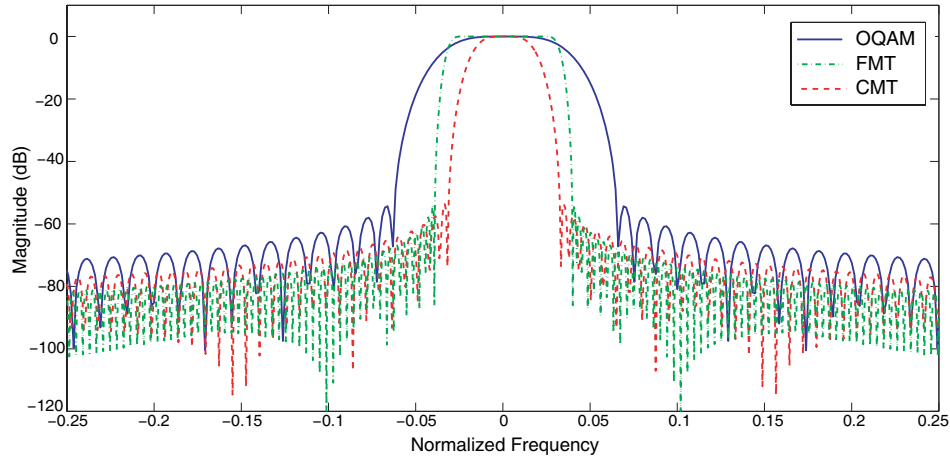


Fig. 6. Comparison between CMT and OFDM-OQAM prototype filters

characterized by a constant (complex) gain. Accordingly, at the receiver, distortion can be compensated in each subcarrier band by applying a single-tap equalizer whose gain is the inverse of the channel gain. The same is true in filterbank-based multicarrier communication systems. Here, by reducing the width of each subcarrier band (through increasing the number of subcarriers, N), subcarrier channels can be modeled as narrow-band, non-frequency selective channels. As a consequence, here also, equalization becomes trivial and can be performed through a single-tap equalizer.

7. CONCLUSION AND OUTLOOK INTO FUTURE RESEARCH

We discussed and compared OFDM-OQAM, CMT and FMT as multicarrier communication techniques for CR systems. We derived the orthogonality condition for OFDM-OQAM and showed that of all multicarrier methodologies, for a fixed filter length, OFDM-OQAM achieves the highest stopband attenuation. However, while inferior in terms of spectral leakage, CMT offers better frequency selectivity. For both methods, more research is necessary to quantify the effects of imperfect timing phase and carrier recovery on system performance.

8. REFERENCES

- [1] P. Amini, R. Kempter, R. R. Chen, L. Lin and B. Farhang-Boroujeny, "Filter Bank Multitone: A Physical Layer Candidate for Cognitive Radios," Software Defined Radio Technical Conference, SDR 2005, November 14-18, 2005.
- [2] B. Farhang-Boroujeny and R. Kempter, "Multicarrier Communication Techniques for Spectrum Sensing and Communication in Cognitive Radios," submitted to IEEE Communications Magazine
- [3] T.A. Weiss and F.K. Jondral, "Spectrum Pooling: An Innovative Strategy For The Enhancement Of Spectrum Efficiency," IEEE Communications Magazine, Vol. 42, No. 3, March 2004, pp. S8 - S14.
- [4] T.A. Weiss, J. Hillenbrand, A. Krohn, and F.K. Jondral, "Mutual Interference In OFDM-Based Spectrum Pooling Systems," IEEE 59th Vehicular Technology Conference, VTC 2004-Spring, 2004, vol. 4, May 17-19, pp. 1873 1877.
- [5] Federal Communications Commission, "Spectrum Policy Task Force," rep. ET Docket no. 02-135, Nov. 2002
- [6] R.W. Chang, "High-speed Multichannel Data Transmission With Bandlimited Orthogonal Signals," *Bell Sys. Tech. J.*, vol. 45, pp. 1775-1796, Dec. 1966.
- [7] B.R. Saltzberg, "Performance of an Efficient Parallel Data Transmission System," *IEEE Transaction on Communication Techniques*, vol. 15, no. 6, pp. 805-811, Dec. 1967.
- [8] B. Hirotsaki, "An Orthogonally Multiplexed QAM System Using the Discrete Fourier Transform," *IEEE Transactions on Communications*, Volume 29, Issue 7, Jul 1981 Page(s): 982 - 989
- [9] M. Bellec, P. Pirat, "OQAM Performances And Complexity," 802.22 contributions, doc., IEEE 802.22-06/0004r0
- [10] G. Cherubini, E. Eleftheriou, S. Olcer, J.M. Cioffi, "Filter Bank Modulation Techniques For Very High Speed Digital Subscriber Lines," *IEEE Communications Magazine*, vol. 38, no. 5, pp. 98-104, May 2000.
- [11] G. Cherubini, E. Eleftheriou, S. Olcer, "Filtered Multitone Modulation For Very High-Speed Digital Subscriber Lines," *IEEE Journal on Selected Areas in Communications*, vol. 20, no. 5, pp. 1016-1028, June 2002.
- [12] G. Cherubini, E. Eleftheriou, S. Olcer, "Filtered Multitone Modulation for VDSL," in *Proc. IEEE Globecom 99*, vol. 2, pp. 1139-1144, 1999.
- [13] S.D. Sandberg and M.A. Tzannes, "Overlapped Discrete Multitone Modulation for High Speed Copper Wire Communications," *IEEE Journal on Selected Areas in Communications*, vol. 13, no. 9, pp. 1571-1585, Dec. 1995.
- [14] B. Farhang-Boroujeny, "Multicarrier modulation with blind detection capability using cosine modulated filter banks," *IEEE Transactions on Communications*, vol. 51, no. 12, pp. 2057-2070, Dec. 2003.
- [15] L. Lin and B. Farhang-Boroujeny, "Cosine modulated multitone for very high-speed digital subscriber lines," EURASIP, Accepted for publication.
- [16] Rossi, M., Jin-Yun Zhang, Steenaart, W., "Iterative least squares design of perfect reconstruction QMF banks," IEEE Canadian Conference on Electrical and Computer Engineering, 1996.
- [17] B. Farhang-Boroujeny, "A Universal Square-root Nyquist (M) Filter Design for Digital Communication Systems," Software Defined Radio Technical Conference, SDR 2006, November 13-17, 2006